Risinoleaic Acid Derivates as Templates for Synthesis of Mesoporous Silica Material based on Tetraethylorthosilicate and 3-Aminopropyltrimethoxysilane as CO-Structure Directing Agent

Andriyani[1*], Marpongahtun Y. Muis[1]

[1]*Department of Chemistry, Faculty of Matematics and Natural Science, Universitas Sumatera Utara, Medan, Indonesia*

Keywords: FT-IR, X-ray diffraction, scanning electron microscopy

Abstract: The synthesis of mesoporous silica using sodium risinoleate as a template, 3-aminopropyltrimethoxysilane as the structural directing agent and tetraethylortosilicate as a source of silica was carried out. The reaction conditions are carried out by varying the amount of silence before the aging stage. Mesopore silica obtained was characterized using FT-IR, X-ray diffraction (XRD), scanning electron microscopy (SEM) and porosity analysis.

1 INTRODUCTION

Synthesis of silica material using tetraethyl orthosilicate (TEOS) as a silica source takes place through a sol gel process with several steps: (i) hydrolysis and condensation of precursor molecules and sol formation, (ii) gelatinization (gel sol transition), (iii) aging and (iv) drying (Schubert & Husing, 2005). The hydrolysis stage and condensation to sol gel are affected by acid or base conditions. Silica material which has pores is obtained by adding organic components in the form of supramolecules such as surfactants or biomacromolecules which function as templates. Pores in the material will be obtained after the organic components are removed by calcination.

The formation of mesoporous silica material which has a pore size between 2-50 nm using surfactant as a template through the Cooperative self-assembly route beginning with the formation of nuclei in the liquid solution system of surfactants with inorganic components, then the nuclei undergo incorporation to form aggregates so that a solid phase is formed which is separated from the liquid phase. Furthermore, polymerization and condensation of inorganic materials occur. Through the calcination process mesopore material will form (Wan, 2007).

The interaction between organic matter (surfactants) and inorganic materials (silica precursors) greatly determines the pore characteristics obtained. The use of anionic surfactants with a negative charge on the head group (S^-) and cationic surfactants with a positive charge on the head group (S^+) in the formation of mesostructural material is regulated through electrostatic interactions. Interaction can occur directly in the form of S^+I^- and S^-I^+ (I inorganic components) or indirectly using bridges with ion counterparts such as halogen anions ($X^- = Cl^-$, Br^-) with the interaction of $S^+X^-I^+$ and $S^-X^+I^-$ takes place in acidic and alkaline cations ($M^+ = Na^+$, K^+ with $S^-M^+I^-$ interactions in alkaline conditions (Soler-Illia G J et al, 2002). Mesostructural synthesis using anionic surfactant with route (S-I +) produces hexagonal mesostructures and lamellar copper oxides and by route ($S^-M^+I^-$) produces lamellar zinc oxide (Huo, 1994). The use of anionic surfactants as templates is difficult to get good interaction between silica and surfactants. The use of organosilan as a co-structure-directing agent (CSDA) to achieve good interaction between surfactants and inorganic species has been proposed by (Che, 2003). The structure of the organosilan compound contains two sides of the alkoxilane which can condense with silica precursors (TEOS) and the organic side which can form electrostatic, covalent, hydrogen bonds or π-π interactions with surfactant head groups. Bridges of organic and inorganic species will help self-organization into regular assemblies.

Synthesis of various mesoporous silicates (AMSn) using N-lauryl glutamic acid and aminopropyl triethoxysilane (APS) as co-structure directing agents (CDSA) and tetraethyl orthosilicate has been carried out (Gracia, 2005). Synthesis of AMS 0.5 was carried out using sodium dodecyl sulfate (SDS) in water / ethanol followed by the

addition of a mixture of surfactants 3-aminopropyl triethoxysilane (APTES) and tetraethyl silicate (TEOS) (Yokoi, 2003).

Risinoleic acid (12-hydroxy-9-cis-octadecenoic acid, $C_{18}H_{34}O_3$) is an unsaturated fatty acid found in the seeds of the Castor plant (*Ricinus cmmunis L., Euphorbiaceae*). Industrially, ricinoleic acid is produced from safonification or fractionation distillation from castor oil hydrolysis. Risinoleic acid in the form of salt can be sodium risinoleate ($C_{18}H_{33}NaO_3$) in the form of pale white flour, while in the form of methyl esters risinoleic acid ($C_{19}H_{36}O_3$) in the form of a paleyellow liquid. In previous studies we have examined the effect of variations in 0.1N hydrochloric acid in the synthesis of mesoporous silica materials using sodium risinoleic salt as a template (Andriani, 2013). In this paper, we will report the synthesis of silica mesoporous material using derivates of ricinoleic acid, namely sodium risinoleate as a template by varying the amount of silting time before the aging stage. Also synthesized mesoporous silica material using methyl ester risinoleate as a template by adding methanol as cosolvent.

2 RESEARCH AND METHOD

2.1 Material

Tetraethylorthosilicate (TEOS, 98%) and 3-aminopropyltrimethoxysilane (APMS) and hydroclhoric acid were purchased from Sigma Aldrich, sodium ricinoleic acid (C18H33NaO3) obtained from VWR, and deionized water obtained from pt sumber aneka karya abadi.

2.2 Material

Tetraethylorthosilicate (TEOS, 98%) and 3-aminopropyltrimethoxysilane (APMS) and hydroclhoric acid were purchased from Sigma Aldrich, sodium ricinoleic acid ($C_{18}H_{33}NaO_3$) obtained from VWR, and deionized water obtained from PT Sumber Aneka Karya Abadi.

2.3 Characterizations

The obtained products were then subjected to characterization by using X-ray diffraction (Philip PW 1710), Fourier transform infrared (Shimadzu IR-Prestige-21), scanning electron microscope (JEOL JSM-7000F and ZeissVPSEM1555), transmission electron microscope (JEOL JEM-1400), and adsorption desorption isotherm (Quantachrome Auto-sorb).

2.4 Synthesis of Silica Mesopurus Material using Sodium Ricinoleic Acid as Template, 3-aminopropyltrimehoxysilane (APMS) as CSDA, tetraethylorthosilicate (TEOS), Methanol and Variasi Pendiaman (statically) Sebelum Pematangan

Sodium ricinoleic acid 2.072 g (6.47 x 10^{-3} mol) and 210 ml deionized water was added into a two-neck flask and stirred. Into the mixture was then added 8.4 g (7.06 x 10^{-4} mol) HCl 0.1 M and stirred 1 hour at room temperature (solution A). A mixture of 9.8 g (0.047 mol) tetraethylorthosilicate and 0.7 g (0.022 mol) 3-aminopropyltrimethoxysilane in 0.7 g (0.022 mol) methanol were prepared in another beaker and stirred for 15 minutes (solution B). The solution B was added into solution (A) and stirred for another 2 hours at room temperature. The mixture was cured in an oven at a temperature 80°C for 45 hours. A white precipitate was separated from the solution by centrifuge and washed with deionized water and dried at 50°C. Surfactant was then removed by calcination at 550°C for 6 hours. The above process was repeated with time variation of statically treatment at 1 and 2 hours and without statically. The obtained products were then subjected to characterization by using X-ray diffraction (XRD), FT-IR, SEM and TEM and adsorption desorption isotherm (Quantachrome Auto-sorb). The conditions reaction can be seen in Table 1 below.

Tabel 1: Condition of reaction with variation time statically treatment before aging process.

Treatment	Na-risinoleic (mol)	APMS (mol)	TEOS (mol)	HCl (mol)	Metanol (mol)	Statically time(hours)
Run 8b	6.5 x 10^{-3}	3.9 x 10^{-3}	0.047	7.1 x 10^{-4}	0.02	-
Run 9b	4.7 x 10^{-3}	5.6 x 10^{-3}	0.034	1.5 x 10^{-3}	0.03	1

Tabel 1: Condition of reaction with variation time statically treatment before aging process. (cont.)

Treatment	Na-risinoleic (mol)	APMS (mol)	TEOS (mol)	HCl (mol)	Metanol (mol)	Statically time(hours)
Run 10b	4.7 x 10^{-3}	5.6 x 10^{-3}	0.034	1.5 x 10^{-3}	0.03	2
Run 11b	6 x 10^{-3}	7.3 x 10^{-3}	0.085	6 x 10^{-3}	-	2

3 RESULT AND DISCUSSION

3.1 Synthesis of Silica Mesoporous Material using Sodium Ricinoleic Acid as Template, 3-aminopropyltrimethoxysilane as CSDA, tetraethylorthosilicate (TEOS), Methanol and Variations of Standing Time before the Aging Treatment

Synthesis of mesoporous silica material using tetraethylortosilicate, sodium risinoleate, 3-aminopropyl trimethoxysilane with the addition of HCl and methanol was carried out by varying the static time before aging at 80°C. The addition of methanol serves as a co-solvent to homogenize the reaction mixture and can also affect the formation of sodium risinoleic micelles which serve as templates (Wang, 2009).

Silica material at Run 8b before calcination is solid with a soft yellowish white texture. The solids are light yellow due to the mole template ratio of sodium risinoleate and HCl large enough (9:1) and the mole ratio of sodium risinoleate and methanol is quite low (1:3), so that the methanol used is not enough to dissolve excess sodium risinoleate. Solids obtained after calcination are fine white, light and soft solids.

Whereas silica material at Run 9b before calcination is obtained, white solids are slightly harder than Run 8b and have homogeneous fine grains. White solids are obtained due to an increase in the mol ratio of sodium risinoleate to HCl (3: 1) and the mole ratio of sodium risinoleate to methanol (1: 7), an increase in the amount of methanol can dissolve excess sodium risinoleate. After calcination, it is obtained a harder white solid and granular granules.

Silica material from Run 10b before calcination is obtained with a soft soft white solid containing granules or granules. After calcination, white solids are obtained which are harder and have granules larger in size than particles of Run 9b.

Silica material from Run 11b before calcination obtained yellowish white solids and has smaller granules than Run 10b. The solid color is slightly yellow because it does not use methanol even though the mol ratio of sodium risinoleate and HCl is greater (2: 1). After calcination is obtained, a dry creamy white solid has granules finer than Run 10b. All silica materials were characterized using FT-IR, XRD, SEM and porosity analysis.

3.1.1 X-ray Diffraction (XRD)

Analysis of X-ray diffraction (XRD) of silica material products Run-8b, Run-9b, Run-10b, and Run-11b can be seen in Figure 2 below.

Diffractogram of XRD of mesoporous silica material Run 8b, Run 9b, Run 10b and Run 11b (Figure 1) at a 2θ between 10° and 30° indicates that all diffractograms have the same shape as a broad peak around 24.0°. This proves that the material is amorphous and has nanoparticle size. This is consistent with the data reported by previous researchers (Li B, 2011)(Zao Q, 2011)(Zhang J, 2003)(Shah, 2009)(Khali, 2007)(Lin, 2010)(Park, 2006).

All silica material obtained in Run 8b, Run 9b, Run 10b and Run 11b (Figure 2) shows the widened absorption peaks between 3638 cm^{-1} to 3167 cm^{-1}, this is due to the strain of OH (Si-OH) groups, while at 965 cm^{-1} to 951 cm^{-1} is given by Si-OH asymmetric group (υ_{as} Si-OH). Other absorption peaks were also seen at 1107 cm^{-1} to 1094 cm^{-1} which were sharp due to the presence of Si-O-Si asymmetric group (υ_{as} Si-O-Si) and at 804 cm^{-1} to 801 cm^{-1} caused by the presence of a Si-O-Si symmetrical group (υ_s Si-O-Si). Infrared spectrum data obtained for Run-8b, Run-9b, Run-10b and Run-11b are all supported by literature data (Khali, 2007)(Liu H, 2007)(AlOthman, 2010)(Zhao, 2011).
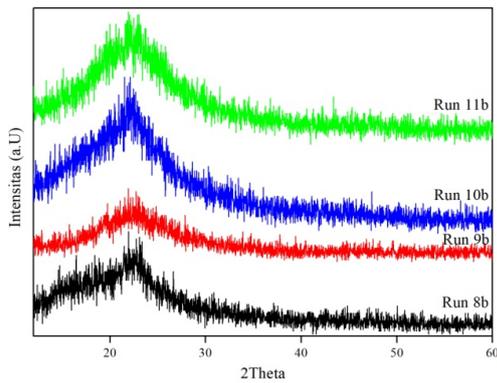
Figure 1: Diffractogram of XRD silica material Run 8b, Run 9b, Run 10b and Run 11b

3.1.2 FT-IR Spectroscopy

FT-IR spectrum of silica material from Run 8b, Run 9b, Run 10b, and Run 11b can be seen in Figure 2 below.
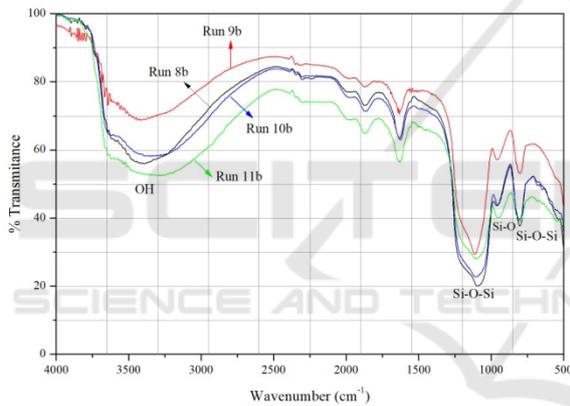
Figure 2: FT-IR spectrum for silica material Run 8b, Run 9b, Run 10b and Run 11b.

3.1.3 Scanning Electron Microscope (SEM)

Morphological analysis of mesoporous silica material Run 8b, Run 9b, Run 10b and Run 11b are carried out with SEM photos with magnifications between 2000X to 25,000X. SEM images are shown in Figure 3 below.
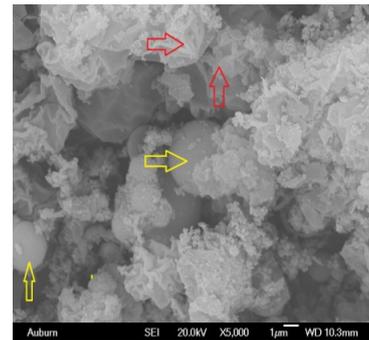
(a) Run 8b (5000X magnification)
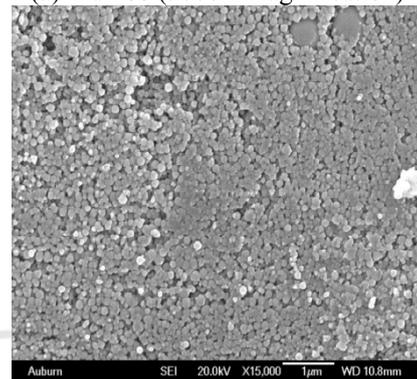
(b) Run 9b (15,000X magnification)
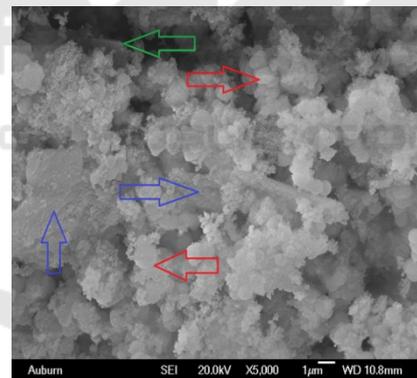
(c) Run 10b (5000X magnification)
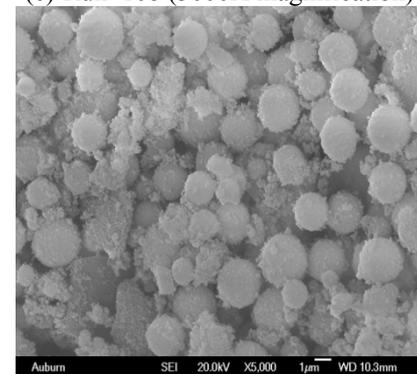
(d) Run 11b (5000X magnification)

Figure 3: SEM image of silica mesopori material: (a) Run 8b; (b) Run 9b; (c) Run 10b and (d) Run 11b.

SEM image of silica material Run 8b (Figure 3a) with 5000 times magnification shows the material has a particle shape in the form of a mixture consisting of dispersed spherical spherical particles (⇨ sign) and particles in the form of thin sheets that blend together to form wrinkled roundabouts and multiples (sign ⇨). There are also particles that have thin skin / walls that are susceptible to damage forming sheets (Liu H, 2010)

SEM photo of silica material Run 9b with a magnification of 15,000 times (Figure 3b) shows spherical particles of small size having a uniform shape to form together to form a tight and compact surface so that there are no gaps between particles. An increase in the ratio of the amount of methanol added seems to have an effect on particle size. The particle size of Run 9b is smaller than the particle size of Run 8b. SEM image of silica material Run 10b with 5000 times magnification (Figure 3c) shows spherically shaped particles forming an aggregate (⇨ sign) and also there is a particle shape in the form of large chunks (⇨ sign) and between particles there is a gap (⇨ sign).

SEM image of silica material Run 11b with 5000 times magnification showing spherical particle shape that is uniform in shape and dispersed with a more perfect particle shape. Particle size is greater than particle size Run 9b and Run 10b.

3.1.4 Adsorption-desorption Isotherm Nitrogen

Porosity analysis of mesoporous silica material and pore size distribution of Run 8b, Run 9b, Run 10b and Run 11b were carried out by desorption nitrogen analysis with isotherm at -196°C. The isotherm adsorption graph was calculated using the Brunauer-Emmet-Teller (BET) method (Figure 4) and the pore size distribution was calculated using the Barret-Joyner-Halenda (BJH) method (Figure 5). Based on Figure 4, the desorption isotherm adsorption chart from Run 8b (black graph) shows a graph of desorption of Type IV adsorption isotherms according to the IUPAC classification, this is also adjusted to the literature (Khalil, 2007). The type of loop hysteresis is caused by the pores in the non-turbulent aggregate of the particles which results in slit-shaped pores according to the literature (Shah, 2009). While the desorption adsorption isotherm graph from Run 9b (red graph) shows Type IV desorption isotherm adsorption according to the IUPAC classification is characteristic for mesoporous material (Khalil, 2007). The existence of a hysteresis loop is due to the narrow pore gap and includes the

pore of the micropore region, according to the literature (Shah, 2009). The adsorption isotherm adsorption graph from Run 10b (blue graph) shows adsorption of Type IV isotherm according to the IUPAC classification which is characteristic for mesoporous material (Khalil, 2007). Pore adsorption is a type of capillary condensation having a hysteresis loop which can be caused by channels such as cylinders or pores formed from coarse homogeneous spheres forming tight agglomerates according to the literature (Shah, 2009). Then the adsorption desorption graph isotherm Run 11b (green graph) shows adsorption of Type IV isotherm according to the IUPAC classification which is a characteristic of mesoporous material (Khalil, 2007). The presence of a hysteresis loop can be caused by pores formed from pore channels such as cylinders or pores from coarse homogeneous sphere particles according to the literature (Shah, 2009).
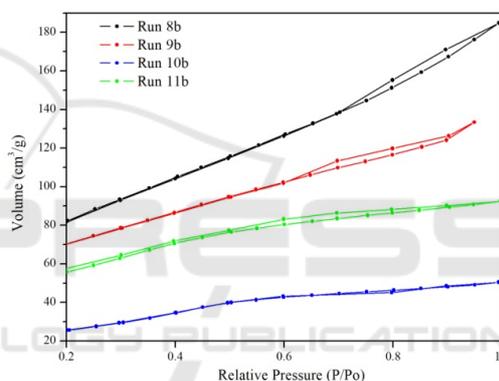
Figure 4: Adsorption desorption graph isotherm nitrogen silica material from Run 8b, Run 9b, Run 10b and Run 11b.

Based on Figure 5, a graph of the pore size distribution of silica material Run 8b (black graph) shows a non-uniform pore size distribution in the range between 1.44 nm to 9.53 nm, this is according to SEM analysis. Mesopore silica material consists of mixed particle forms so produced various pore shapes. The pore size distribution chart of the silica material Run 9b (red graph) shows that the pore size distribution is not uniform from 1.43 nm to 9.53 nm. This is in accordance with SEM photos that show the form of particles that combine to form a compact and tight surface. The particle size distribution chart of silica material Run 10b (blue graph) shows a regular pore size distribution (uniform) dominated by pore size at 2.76 nm and 3.07 nm. This is consistent with SEM photos where dominant particles are spherically shaped in small sizes. The pore size distribution chart for silica material Run 11b (green graph) shows a

uniform pore size and is dominated by 2.45 nm. This is consistent with the results of SEM photos showing the presence of spherical particles that have a uniform and dispersed size.
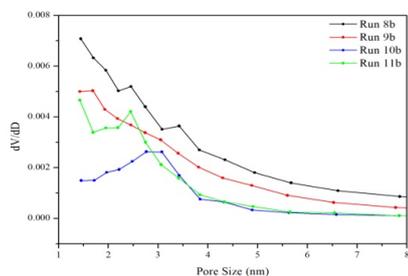
Figure 5: Pore size distribution graph of silica material Run 8b, Run 9b, Run 10b and Run 11b.

Porosity of mesoporous silica material Run 8b, Run 9b, Run 10b and Run 11b such as diameter and pore volume and surface area tabulated in Table 2 below.

Table 2: Diameter, pore volume and surface area of mesoporous material from Run 8b, Run 9b, Run 10b and Run 11b.

Treatment	Pore diameter (nm)	Pore Volume (cm^3/g)	Surface Area (m^2/g)
Run 8b	1.5-9.5	0.02-0.22	54-301
Run 9b	1.4-9.5	0.02-0.16	58-240
Run 10b	3.1	0.04	66
Run 11b	2.5	0.05	113

4 CONCLUSIONS

Synthesis of silica mesoporous material from tetraethylortosilicate (TEOS) as a source of silica, sodium risinoleate as template and 3-aminopropyltrimethoxysilane (APMS) as co-structure directing agent (CDSA) was carried out. The results of the FT-IR analysis proved that tissue was formed (-Si-O-Si-) and the results of XRD analysis were all amorphous material. The variation of calming time before the aging stage produces silica material with different morphology. Porosity analysis of silica material which has a more uniform pore size resulted from treatment with time of drying for 2 hours before the aging stage (Run 10b) and the addition of methanol without the addition of hydrochloric acid (Run 11b) with a pore size distribution of 3.1 nm respectively and 2.5 nm.

ACKNOWLEDGMENT

REFERENCES

Schubert U and Husing N 2005 *Synthesis of Inorganic Materials* (Wiley-VCH Verlag GmbH & Co, KGoA, Weinheim) p 308-309

Wan Yand Zhao D 2007 *Chemical Rev.* 7(**107**): 2821-2860

Soler-Illia G J et al 2002 *Chem. Rev.* (**102**): 4093-4138

Huo Qet al 1994 *Nature* (**368**): 317-321

Che S et al 2003 *Nature Material* (**2**): 801-805

Garcia-Bennett A E 2005 *Angew. Chem. Int. Ed.* (**44**): 5317–5322

Yokoi T et al 2003 *Chem. Mater.* 15 (**24**): 4536-4538

Andriayani et al 2013 *Advanced Material Research* (**789**): 124-131

Wang W Q 2009 *Journal of Colloid and Interface Science* (**331**): 156–162

Li B et al 2011 *Journal of Colloid and Interface Science* (**362**): 42-49

Zhao Q et al 2011 *Applaid surface Science* (**257**):2436-2442

Zhang J Z et al 2003 *Self-Assembled Nanostructure* (Kluwer Academic Publishers, New York) p

Shah A T et al 2009 *Journal of Colloid and Interface Science* (**336**):707-771

Khali K M S 2007 *Journal of Colloid and Interface Science* (**315**):562-568

Liu H et al 2010 *Journal of Colloid and Interface Science* (**346**):486-493

Park Y et al 2006 *Journal of Colloid and Interface Science* (**295**):464-471

AlOthman Z A and Apblett A W 2010 *Applied Surface Science* (**256**):573-3580

Zhao Q et al 2011 *Applaid surface Science* (**257**): 2436-2442

Liu H et al 2010 *Journal of Colloid and Interface Science* (**346**):486-493

Khalil K M S 2007 *Journal of Colloid and Interface Science* (**315**):562-568

Shah A T et al 2009 *Journal of Colloid and Interface Science* (**336**):707-771

Gregg S J and Sing K S W 1982 *Adsorpsi, Surface Area and Porosit* (Academic Press, Second Edition, London (LDT) p

Rouqe-Malherbe R M A 2007 *Adsorption and Diffusion in Nanoporous Materia* (CRC Press Taylor & Francis Group) p